On-Demand Transformation of Carbon Dioxide into Polymers enabled by comb shaped metallic oligomer catalyst

Han Cao[1,2], Ruoyu Zhang[1,2], Zhenzhen Zhou[1,2], Shunjie Liu[1,2], Youhua Tao[1,2], Fosong Wang[1,2], and Xianhong Wang[1,2*]

[1] Key Laboratory of Polymer Ecomaterials, Changchun Institute of Applied Chemistry, Chinese Academy of Sciences, Changchun, 130022, China

[2] University of Science and Technology of China, Hefei, 230026, China

e-mail: xhwang@ciac.ac.cn

Abstract:

Quantitative transformation of CO_2 can greatly elevate the sustainability impact of CO_2 chemical utilization, but it is formidably challenging due to the sluggish kinetics requiring overwhelmingly excess usage of CO_2. Here, we report an on demand CO_2 transformation by a switch polymerization method, *that is*, all reactants including CO_2 are fully converted without any by-product, generating tailor-made poly(ether carbonate) polyols (CO_2-polyols) whose composition and chain length exactly correspond to the feed of CO_2, epoxide and diacid. This is the first time for CO_2 as a countable monomer which is in most cases obscurely considered as "pressure condition". Studies on the kinetics rate law and the activation parameters of key intermediates disclose that it is the multisite cooperativity from metallic oligomer catalyst that facilitates quantitative insertion of CO_2 into polymer backbone without adverse backbiting throughout the polymerization. Hence, this work not only introduces the conception of quantitative CO_2 transformation, but engineers exquisite CO_2-based polymer which is rarely achieved.

Keywords: quantitative, CO_2 transformation, CO_2-polyol, oligomer catalyst, precise catalysis

Introduction

Chemical conversion of CO_2 offers a promising avenue to valorize the waste "greenhouse" gas and deviate the reliance of chemical synthesis on fossil fuel feedstocks, thus creating a more sustainable carbon economy.[1,2] However, the common high pressure reaction condition results in low CO_2 conversion, leading to either the discharge of trouble-some CO_2 to the atmosphere, or the cumbersome energy input CO_2 recycle. To date, only few reactions can theoretically consume CO_2 in quantitative yield, such as catalytically irrelevant mineral carbonation[3] and amines to absorb CO_2 and generate carbamate.[4] But quantitative CO_2 transformation is scarcely reported in sophisticated CO_2 catalysis such as various CO_2 reduction reactions to afford fuels and bulk chemicals,[5,6] and non-redox coupling reactions for cyclic carbonate and polymer production.[7-9] The product yield or the conversion of economically valuable reactants is at the center of these research fields while CO_2 conversion is neglected and hardly studied on a mole basis. In this context, we are wondering whether CO_2 could be quantitatively consumed in these advanced CO_2 chemical transformations.

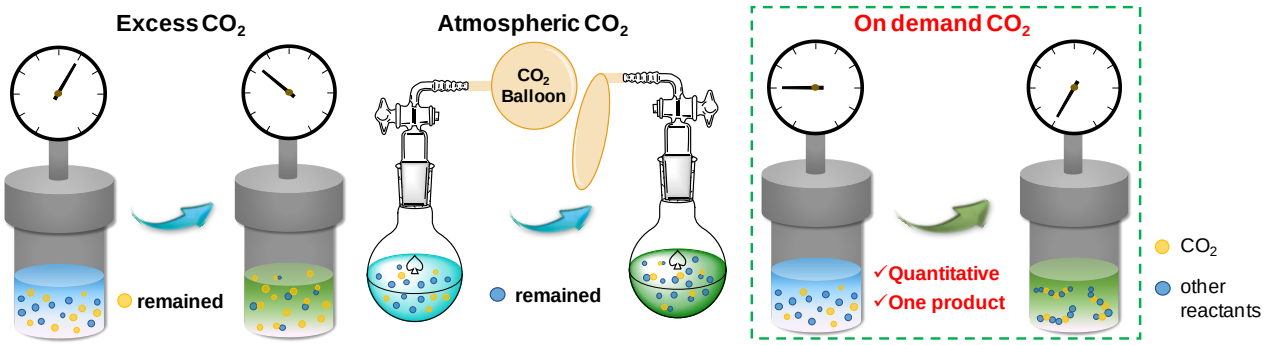

Figure 1. Conceptual blueprint of on demand CO_2 transformation.

Technically, quantitative transformation of CO_2 can be simply achieved by just feeding less. Taking the cycloaddition reaction as example, ambient pressure CO_2 can be fully reacted with largely excess epoxide, which obviously puts the cart before horse as the great surplus of carbon-containing compounds.[10] Meanwhile, the increased conversion in CO_2 reaction can also diminish otherwise well-controlled selectivity and thus form undesired product distribution.[11] Energy required in product separation leads to extra CO_2 production. Therefore, simple full consumption of CO_2 without strict criteria is not the objective here. Instead, what we desire to establish is a comprehensive scenario which lets all reactants serve their proper purpose. That is, an on demand CO_2 transformation is proposed which is different from both the lavish high-pressure reaction, and also the pursuit of absolute ambient pressure reaction (Fig. 1). The term "on demand" here refers to: 1) complete conversion of every involved reactants and 2) only one product formed. Such scenario of "make the best use of everything" renders CO_2 catalysis in line with the principles of green chemistry to a larger extent.[12]

In this work, we successfully fulfill the on demand CO_2 transformation by virtue of the catalytic chain-transfer polymerization of CO_2 and propylene oxide (PO). The reaction that generates cutting-edge CO_2-derived product the poly(ether carbonate) polyol,[13-15] provides a platform for our proposal from three perspectives: for reaction formula, n CO_2 molecules are fixed as carbonate linkage via ring-opening copolymerization (ROCOP) with equivalent POs, and ring-opening polymerization (ROP) of remained m POs form ether linkage; for mechanism, the insertion of CO_2 is fast and zero-order dependent in rate law;[16-18] for reaction system, the soft ether linkage and the nature of formed low-molar-mass polymer allow the full conversion without the restriction from viscosity. Notwithstanding the theoretical viability, such "on demand" CO_2 transformation via polyol route is challenging from catalyst. State-of-the-art CO_2/epoxide ROCOP catalysts, either stringently afford carbonate linkage which gives rise to solidified medium limiting full conversion,[19-21] or only exhibit activity at harsh condition inducing high proportion of CO_2 in the gas phase and side-reaction.[22-24] To address this issue, we adopt a comb shaped metallic oligomer catalyst **CAT 1** comprising multiple functionalized Al(III) porphyrin complexes at the side chain. Owing to the unique multimetallic synergistic catalysis, **CAT 1** exhibits fast and comparable ROCOP and ROP rate with unprecedented selectivity, which quantitatively converts PO and CO_2 into CO_2-polyols as the sole and only target in a switch catalysis manner (Fig. 2). This proof-of-concept study offers a fresh perspective on precisely handling CO_2 in reactions and also a more convincing blueprint of sophisticated CO_2 catalysis as a potential toolbox for future carbon reduction.

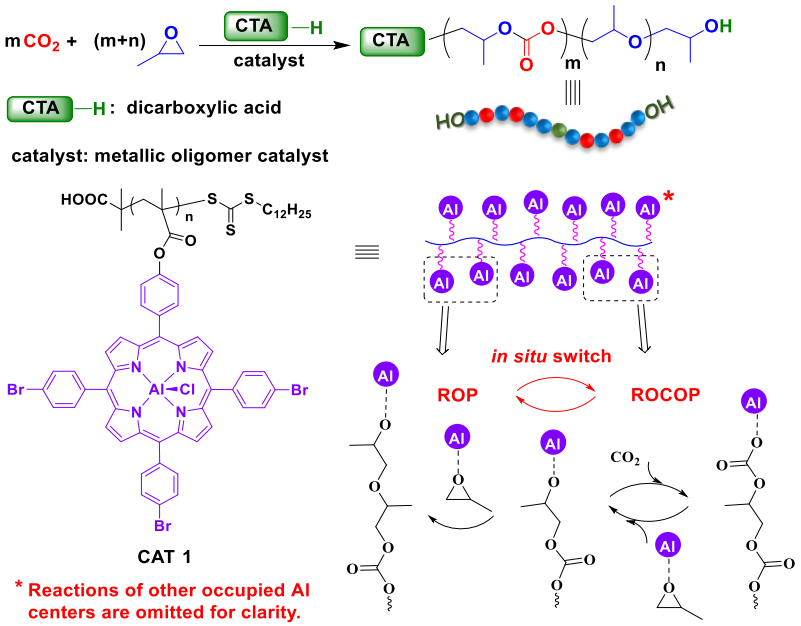

Figure 2. On demand CO_2 transformation realized in the chain-transfer polymerization of epoxide and CO_2 using a comb shaped metallic oligomer catalyst (**CAT 1**).

Results and discussion

Tentative attempt

The first objective of our approach is screening catalyst that enables to polymerize CO_2 and excess PO to polyols in full conversion without any by-product, *i.e.* on demand transformation. The by-product refers to cyclic propylene carbonate (cPC) which is often generated in PO/CO_2 ROCOP reaction. The first candidate is double metal cyanide (DMC) solid catalyst pertain to large-scale synthesis of poly(ether carbonate) polyols.[22,23] However, literatures report that it often operates under high pressure (> 2MPa) and temperature (> 80°C) unable to assure full conversion of CO_2. Alternatives are discrete molecular ROCOP catalysts. Some of them are active at low and even ambient CO_2 pressure, but whether quantitative conversion is achievable has not been distinctly demonstrated.[25,26] In our initial hypothesis, although these catalysts in priority alternatively copolymerize PO with CO_2, full monomer enchainment can be realized provided switch catalysis occurs from ROCOP to PO ROP in substoichiometric CO_2 feed. Thus, we initially test this hypothesis using Al(III) porphyrin complex (**mono 1**) by monitoring its whole kinetics profiles with 1.0 MPa CO_2 feed (substoichiometric) and comparing to those with excess CO_2 (3.5 MPa).

According to aliquot ^{1}H NMR analysis (Fig. 3a), the stoichiometry of CO_2 did not influence the rate since the conversion of PO was basically synchronous in the two reactions, however in sharp contrast, the reaction at 3.5 MPa only generated *Ca.* 3 wt% of cPC in invariant selectivity with time while the reaction at 1.0 MPa displayed two distinct stages. When CO_2 is sufficient, the selectivity towards cPC/polyol showed similar with that at high pressure. However, huge amount of cPC (24 wt%) was somehow generated in the end. It was calculated that the ratio of fixed CO_2 in polyols and cPC was 1/1.38 implying the big sacrifice towards selectivity only for the purpose of exhausting CO_2. A separate study using *in situ* infrared spectroscopy disclosed that at high CO_2 conversion the hypothesized switch catalysis did not occur (Fig. 3b-c). The major reaction was polyols depolymerizing to cPC via back-biting while the switch to ROP was the minority. As shown in Table S1, single-site Al(III) porphyrin catalysts were failed to our goal regardless of the

variation of substitution in the porphyrin ligand. Moreover, similar result was also observed using Co(III) salen catalyst (Table S1, Entry 5).[20] Thus, initial attempts using common mononuclear catalysts were unsuccessful.

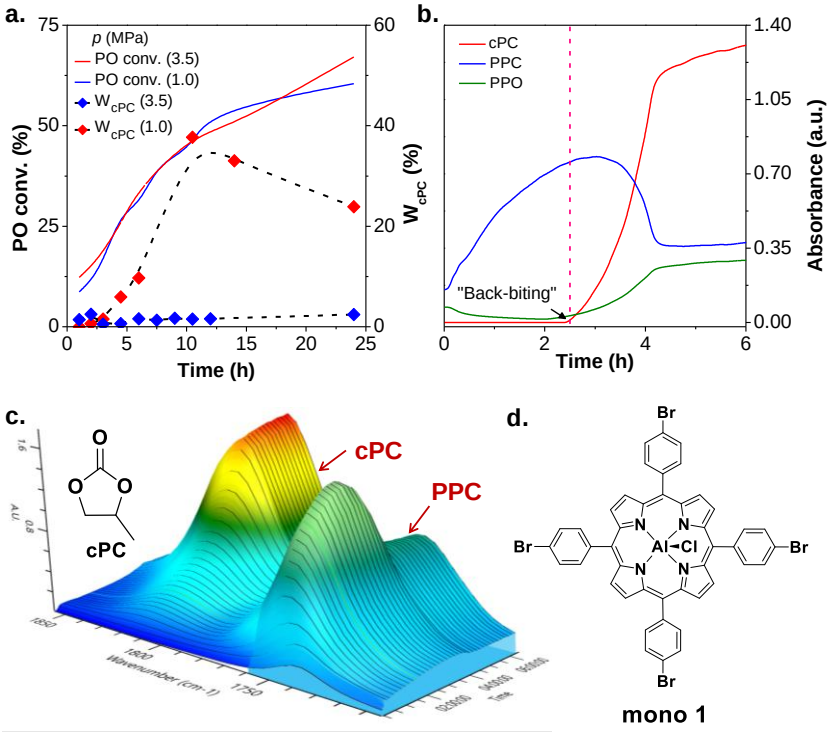

Figure 3. Monitoring quantitative CO_2 polymerization catalyzed by mononuclear complex (**mono 1**). **a.** PO conversion and cPC content in polyols, monitored by *ex situ* aliquot ^{1}H NMR analysis. Reaction conditions: PO/[mono 1]/PPNCl=2500/1/1& PO/SA=30 (molar ratio), 70 °C, 1.0 MPa/3.5 MPa CO_2 pressure. The details are listed in Fig. S2-S5. **b** and **c**. Reaction profiles monitored by *in situ* IR and the resulting three-dimensional stack plot of the IR spectra. Profiles of the absorbance at *Ca.* 1800 cm^{-1} corresponds to ν(C=O) from cPC. Profiles of the absorbance at *Ca.* 1745 cm^{-1} corresponds to ν(C=O) from linear carbonate (PPC) and C=O from ester (formatted from SA) in polyols. Profiles of the absorbance at *Ca.* 1104 cm^{-1} corresponds to ν(C-O) from ether (PPO) in polyols. Reaction condition: PO/[SA]/[mono 1]/PPNCl =2500/50/1/1& PO/SA =30 (molar ratio), 70 °C, 1.5 MPa. **d.** Chemical structure of mono 1.

Metallic oligomer catalyst CAT 1.

With the above results in mind, we consider that the catalyst here should enable 1) fast ROCOP and ROP processes and *in situ* switch between them; 2) excellent protic CTA compatibility for chain-transfer; 3) permanent prevention of backbiting side-reaction. Recently, our group reported a series of metallic oligomer catalysts composed of *Ca.* 4-7 Al(III) porphyrin complexes at the side chain, which greatly suppressed cPC formation in the copolymerization of PO and CO_2 and yielded high-molar-mass poly(ether carbonate).[27] Relatively, in the presence of 50-100 equivalent water and carboxylic acids, the published **CAT 0** achieved excellent selectivity, generating CO_2-polyols with controllable molar mass and narrow distribution (Table S2). However, as a candidate for our task, its activity no matter for turnover frequency (TOF) or productivity needs further improvement. Like most organometallic catalysts, the molecularly well-defined active sites and tailorable structure permit an incisive mechanism-based performance optimization. In this work, several structural modifications considering the identity and number of organometallic moieties, the main chain and linker constructing the oligomer, were carried out as follows: 1) The bromide was introduced in the *meso*-position of the

porphyrin ring to modulate the Lewis acidity of the metal center.[28] 2) The linker between the porphyrin and the main chain was shortened to facilitate the reaction between metal-monomer and metal-chain end. 3) The number of porphyrins per chain was increased to *Ca.* 12 to further enlarge the multisite cooperativity (Fig. S12). Finally, **CAT 1** was obtained in a four-step synthesis (Fig. S13). Its catalytic performance was distinctly outstanding. At 80 °C, TOF of 9,600 h^{-1} was observed in **CAT 1** catalyzed chain-transfer polymerization of PO and CO_2 in the presence of sebacic acid (SA), which was *Ca.* 40 times higher than **mono 1** under the same condition (Entry 1 vs 7, Table S4). Note that for better comparison with single-site catalysts, TOF was calculated based on the substrate conversion per Al center. By raising temperature to 120 °C, TOF of 17,600 h^{-1} was obtained within 1 h, exhibiting very competitive activity compared with the state-of-the-art organometallic CO_2 polymerization catalysts, such as Al(III) porphyrin[29] and Co(III) salen[11] in a bifunctional fashion, and Mg(II)/Co(II) heterodinuclear complex[25]. For comparison with solid catalyst, the value of productivity is also introduced, based on the production of polyols per gram of catalyst. By controlling the temperature, a productivity of 12.5 (kg polyol g^{-1} $cat.^{-1}$) was achieved for 24 h (Entry 9, Table S4). As for selectivity, **CAT 1** cut down the formation of cPC% below 1% at 80 °C and reduced temperature lead to even lower cPC content. Thus, compared with DMC, **CAT 1** demonstrates similar or improved productivity and distinctly advanced selectivity.[30,31] Hence, the cutting-edge performance of **CAT 1** will support our further exploration on our unfinished work.

CAT 1 mediated quantitative CO_2 polymerization.

The results of **CAT 1** mediated on demand CO_2 transformation via polyol route were shown in Table 1. For selectivity, the formation of cPC was all below 0.5 wt% indicating that the hitherto ineluctable backbiting reaction did not occur. As for conversion, final crude mixture of each run was viscous but flowable liquid rather than waxy solid as a consequence of low molar mass and carbonate ratio, facilitating the complete monomer conversion in such bulk condition. Particularly, for entry 1-12, the pressure reading of autoclave fell to minimum in the end and no CO_2 bubbles left when stirring the crude mixture. By quantitative calculation, the conversion of CO_2 all exceeded 94% (the initial CO_2 usage was recorded by mass for careful calculation). Hence, the nearly complete consumption of both monomers and the afforded polyols as the sole product demonstrated that our proposed on demand transformation was successful. Meanwhile, the above experiments with fast polymerization rate were all conducted at ppm level catalyst concentration, where the molar ratio of [Al]/[PO] was 1/50,000/ that corresponds to [**CAT 1**]/[PO] of *Ca.* 1/600,000. Such low catalyst loading minimizes the organometallic residue and further elevate the sustainability impact of this work from the perspective of green synthesis.

An equally important finding is that on demand transformation of CO_2 in turn favored the precise tuning of polyol composition. As shown in Fig. 4a, there was a good linear fit between the initial ratio of monomers and the composition of the polymer in the quantitative zone, where the carbonate ratio in polyol spaciously ranged from 6.9%-36.8%, one-to-one corresponding to initial CO_2/PO of 0.07-0.39. The threshold of quantitative zone is related to the intrinsic ROCOP/ROP selectivity of **CAT 1** which is discussed later. Remarkably, this is the first time for using CO_2 as a countable monomer to produce polymers with predictable carbonate ratio in the field of CO_2 polymer chemistry. As previously reported by us, the composition of CO_2-polyols was only roughly tuned by the reaction condition since heterogeneous catalysis did not allow precise control.[23,31] In comparison with another previous literature, where similar range of carbonate linkage with Table 1 here was obtained at 90 °C and 15-90 bar CO_2 pressure,[14] **CAT 1** produced CO_2-polyols with much lower energy input, which also coupled with the advance of purification-free towards cPC residue. Currently, CO_2-polyols with less CO_2 uptake are the drop-in solution for replacing the fully petroleum-derived polyether polyols in

the manufacturing of polyurethanes, which is a rare example for CO_2 catalysis already in commercial process.[32] Due to the tunable composition of ether/carbonate, CO_2-polyol retains the traits of polyether polyol such as low viscosity and favorable glass transition temperature (T_g) as well as endows the derived polyurethane more comprehensive material property.[33,34] In this unique on demand transformation, CO_2-consumed synthesis and CO_2-derived products offer mutual benefit for each other, *i.e.*, a CO_2-polyol route can directly realize the quantitative conversion of CO_2, and complete conversion provides a made-to-order synthetic protocol for exquisite CO_2-derived polymer.

Table 1. Results of on demand PO/CO_2 polymerization catalyzed by **CAT 1**

entry[a]	CO_2 ini. [g]	CO_2/ PO[b]	Conv. of PO [%][c]	W_{cPC} [d] [wt%]	TOF [h^{-1}][e]	Carbonate [%][f]	CO_2 in polyol [g][g]	CO_2 fixed [%][g]	M_n[h] [g/mol]	$Đ$[h]
1	1.98	0.07	>99	0.2	2500	6.9	1.96	>99	3200	1.11
2	2.76	0.11	>99	0.1	2500	10.6	2.66	96.3	3500	1.10
3	4.05	0.16	>99	0.4	2500	15.6	3.92	96.8	3500	1.11
4	5.30	0.21	94.5	0.2	2360	22.0	5.23	98.7	3600	1.12
5	5.78	0.23	>99	0.1	2000	22.4	5.63	97.4	3600	1.11
6	6.33	0.25	98.6	0.2	1970	24.6	6.10	96.4	3600	1.11
7	7.37	0.29	>99	0.4	1670	28.9	7.27	98.6	3700	1.11
8[i]	7.20	0.29	>99	0.4	1670	27.5	6.92	96.1	3000	1.10
9[j]	7.04	0.28	>99	0.4	1670	27.1	6.82	96.9	2500	1.11
10[k]	7.29	0.29	>99	0.5	1670	28.4	7.14	97.9	1900	1.10
11	8.89	0.35	>99	0.3	1670	34.1	8.58	96.5	3800	1.12
12	9.81	0.39	95.6	0.4	1590	36.8	9.26	94.4	3800	1.11
13	11.72	0.47	>99	0.2	1250	40.2	10.06	85.8	4000	1.12
14[l]	5.89	0.47	94.8	0.8	590	44.9	5.35	90.8	3900	1.11
15	13.71	0.54	>99	0.4	1250	43.4	10.85	79.1	4000	1.12

[a.] Polymerization reactions were run with molar ratio of [PO]:[SA]:[Al]:[PPNCl] = 50000:1000:1:1, at 50 °C in 40 mL PO in bulk. [b.] Initial molar ratio. [c.] Determined by ^{1}H NMR analysis of crude reaction mixture. [d.] The weight percentage of by-product cPC, determined by ^{1}H NMR analysis. [e.] Turnover frequency, calculated by (mol PO $_{\text{to polyol}}$)/(mol Al × h). [f.] Carbonate fraction in polyols, determined by ^{1}H NMR analysis. [g.] Fixation of CO_2 in polyols (g) = mol PO $_{\text{to polyol}}$ × Carbonate% × 44. [h.] Determined by gel permeation chromatography in CH_2Cl_2 at 35 °C, calibrated with polyethylene glycol standards. [i.] Molar ratio of [PO]/[SA]: 40. [j.] Molar ratio of [PO]/[SA]: 32. [k.] Molar ratio of [PO]/[SA]: 25.6. [l.] Polymerization was run at 50 °C with molar ratio of [PO]:[SA]:[Al]:[PPNCl] = 25000:500:1:1, in a mixture of 20 mL PO and 20 mL CH_2Cl_2.

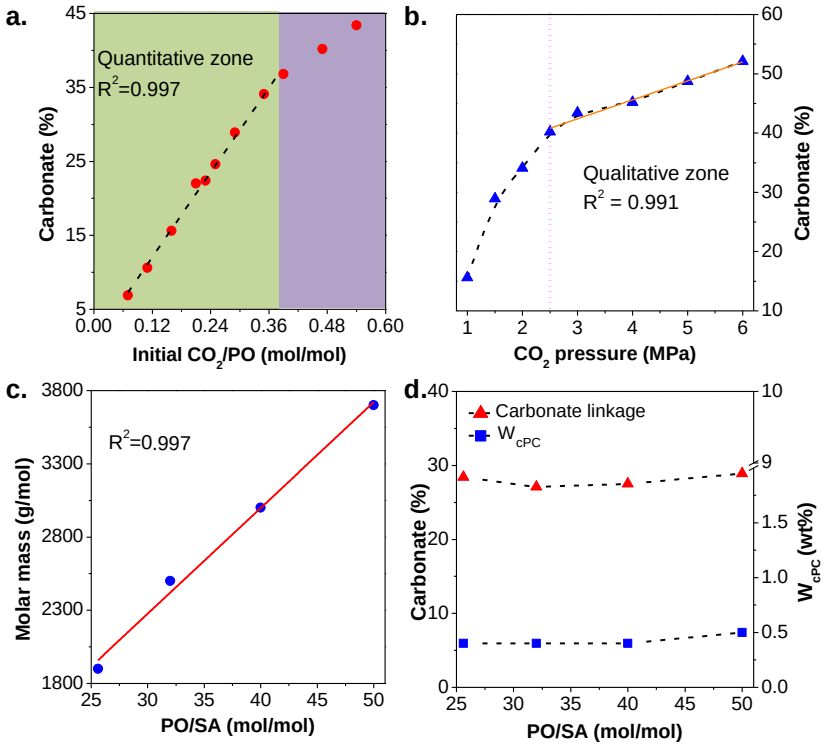

Figure 4. Precisely tuning the structure of CO_2-polyol in the presence of **CAT 1**. **a.** Quantitative relationship between polyol composition and the feed ratio of CO_2/PO. **b.** Qualitative relationship between polyol composition and CO_2 pressure, data were collected from Entry 3, 7, 11, 13, 15 of Table 1 and Entry 1, 2, 3 of Table S6. **c.** Control of molar mass by the feed ratio of PO/SA. **d.** Invariability of selectivity and composition under different ratio of PO/SA. The data of **c** and **d** were collected from Entry 7-10 of Table 1.

The relationship between apparent CO_2 pressure and polyol composition was also studied. At 50 °C, 2 MPa CO_2 pressure relatively corresponds to CO_2/PO molar ratio of 0.35, demarcating the "quantitative zone" (Fig. 4a). The pressure in Entry 13 and 15 of *Ca.* 2.5 MPa and 3 MPa resulted in lower CO_2 conversion (85.8%, 79.1%), while adding solvent can lower the viscosity of the medium and raise the solubility of CO_2, facilitating increased CO_2 conversion (Entry 14, Table 1). In addition, higher pressure *i.e.* excess CO_2 reactions were also investigated (Table S6). CO_2 pressure at 5 MPa raised the carbonate linkage to 48.7%, while a further increase to 6 MPa reached the maximum at 52.1% yet with significant activity loss due to the gas expansion. Interestingly, there is a linear relationship between initial CO_2 pressure and carbonate ratio from 2.5 MPa to 6 MPa, which forms the "qualitative zone". In general, in addition to quantitative prediction, the composition can also be qualitatively predicted by initial CO_2 pressure (Fig. 4b).

Molar mass is another important parameter of CO_2-polyols. Gel permeation chromatography (GPC) analyzed molar mass and distribution were calibrated with polyethylene glycol (PEG) as standards, generally used in characterization of low-molar-mass polyols.[35] As shown in Entry 7-10, Table 1, by altering the amount of SA with fixed CO_2/PO ratio, a series of CO_2-polyols with identical composition, molar mass in the range of 1900-3700 g/mol were delicately prepared accompanied by invariant cPC content (Fig. 4d). The intact catalytic performance illustrated the advanced stability of **CAT 1** while some organometallic catalysts have been reported to undergo deactivation in the presence of excess protic compounds.[36] GPC results showed monomodal and narrow distributions (<1.12) and the molar mass was linearly dependent on the feed of PO/SA with correlation coefficient (R^2) above 0.99, demonstrating the characteristic "immortal" polymerization (Fig. 4c).[37] The as-prepared CO_2-polyols were analyzed by MALDI-ToF mass spectrometry, which

disclosed that all peaks corresponded to poly(ether carbonate) with SA core in the center and hydroxyl functions in terminal (Fig. S35-40). In short, CO_2-polyols can be precisely customized here by adjusting the feed of two monomers and CTA, to meet the different practical requirements.

Kinetics study and mechanistic consideration.

Firstly, we monitored the whole kinetics profiles of CO_2-polyol formation under **CAT 1** using *in situ* infrared spectroscopy. As shown in Fig. 5a, the carbonyl absorption at *Ca.* 1800 cm^{-1} for cPC was absent throughout the reaction. The absorption at *Ca.* 2335 cm^{-1} for CO_2 reached the plateau prior to the absorption at *Ca.* 827 cm^{-1} for PO, which disclosed that the CO_2-involved polymerization directly switched to PO ROP at the late stage. Such *in situ* switch polymerization assured the quantitative CO_2 transformation into polyols, which is sharply differentiated from the occurrence of depolymerization as observed in the mononuclear catalyst. The k_{obs} for carbonate and ether formation determined by the slope of linear part were 0.14 [abs./h] and 0.23 [abs./h], the ratio of which was somehow correlated with the maximum carbonate ratio in the "quantitative zone" (0.14/(0.14+0.23)=0.38). For careful calculation, *ex situ* aliquot ^{1}H NMR analysis was used to determine monomer numbers per chain, CO_2 net fixation and carbonate ratio at different time intervals in two separate reactions at 0.8 MPa/2.2 MPa pressure (Fig. 5b). In the first 6 h of the two reactions, the rate of CO_2 insertion exhibits the same value (*Ca.* 0.4 CO_2 g/h) yet with different carbonate linkage, illustrating the moderate deceleration of PO ROP by the increased CO_2 feed. The 0.8 MPa reaction finished CO_2 consumption within 10.5 h left with 38% unreacted PO and the full conversion of PO was achieved at 20 h. The 2.2 MPa reaction which represented the edge of "quantitative zone", converted 4.6 g CO_2 within 12 h and the rest 0.5 g CO_2 still required another 12 h due to the highly viscous medium. As shown in Fig. 5c, the molar mass increased smoothly with time and displayed monomodal distribution at each time interval with narrow PDI values (<1.14). Meanwhile, the results of GPC analysis fitted well with ^{1}H NMR spectroscopy, demonstrating a well-controlled process. The analysis of molar mass also proved that after CO_2 consumption excess PO continued to insert in the existed chains generating homogeneous poly(ether carbonate) in the end rather than regenerate a sole polyether chain.

In a related research by Williams and coworkers using a mononuclear chromium catalyst, equimolar feed of cyclic anhydride and epoxide formed polyester, while excess epoxide afforded switchable polymerization between ROCOP and ROP producing block copolymers with versatile architectures.[38] Unfortunately, when it came to PO/CO_2, the catalytic cycle was likely to shift to "back-biting" from propagation as illustrated in Fig. 3. In this work, the successful quantitative CO_2 polymerization is undoubtedly attributed to **CAT 1** which shares the same structure of active site with **mono 1** but functions entirely different. To better understand the advanced multisite catalysis of **CAT 1**, we calculated the order in CO_2, epoxide and catalyst for the formation of PPC by determining the initial rates (slopes of absorbance at *Ca.* 1745 cm^{-1} versus time at conversion below 15%) in controlled series of experiments. Since SA with poor solubility in PO, is gradually dissolved by the enchainment of PO, while PEG dissolves well in PO whose absorption at *Ca.* 1104 cm^{-1} flattened very fast as monitored. Therefore, PEG was used as CTA and initial rates were measured without interference. A zero order in CO_2 was observed over the range of 0.5-2.5 MPa pressure, revealing that the insertion of CO_2 is not rate-determining for carbonate formation (Fig. 6a). Surprisingly, the initial rates at 3.0-4.6 MPa were only about one-third of those at 0.5-2.5 MPa due to the gas expansion. As previously reported, CO_2 insertion is always fast and zero-order dependence in most CO_2/epoxide ROCOP catalysis.[16-18] While Rieger and coworkers found that under a di-zinc catalyst the CO_2 insertion was first-order below 2.5 MPa and shifted to zero-order at higher pressure.[39] Similarly, we here found that 2.5 MPa was the boundary between the "quantitative zone" and the "qualitative zone", and yet the distinct shift for

the reaction order in CO_2 was not observed around 2.5 MPa. In the "quantitative zone", the initial rates only fluctuated with CO_2 pressure within the range of ± 13.5%. Therefore, the critical value of the zone also reflected the intrinsic selectivity of **CAT 1** between ROP and ROCOP as disclosed before. In the "qualitative zone", with the increase in CO_2 pressure, the rate of ROP significantly dropped while ROCOP still exhibited the similar rate, which resulted in such coincidentally linear dependency of polyol composition on the CO_2 pressure.

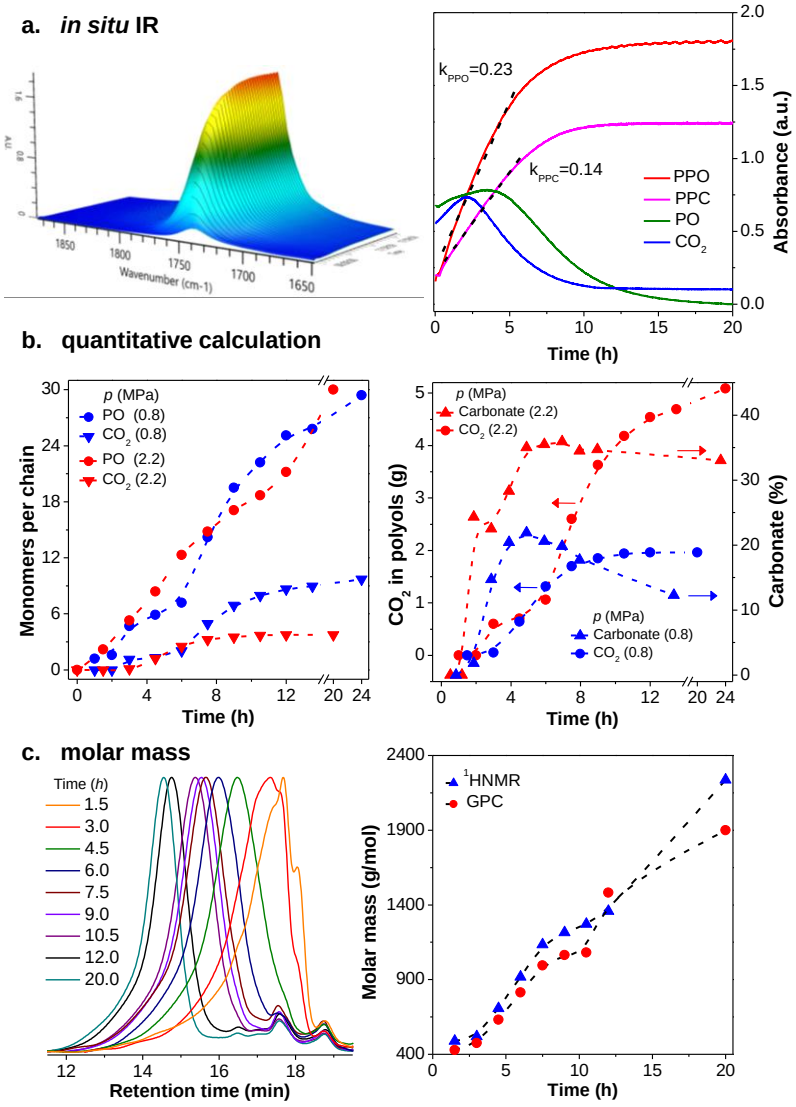

Figure 5. Monitoring **CAT 1** catalyzed quantitative CO_2 polymerization. **a.** Reaction profiles monitored by *in situ* IR and the resulting three-dimensional stack plot of IR spectra. Profiles of the absorbance at *Ca.* 2335 cm^{-1} corresponds to ν(C=O) from CO_2. Profiles of the absorbance at *Ca.* 827 cm^{-1} corresponds to ν(C-O) from PO. Reaction condition: PO/[SA]/[Al]/PPNCl=50000/1000/1/1 (molar ratio), 50 °C, 1.5 MPa CO_2 pressure, 30 mL PO in bulk. The final crude is also determined by ^{1}H NMR analysis: conv. of PO% > 99%, W_{cPC}% 0.2%, Carbonate% 27.1%. **b.** Quantitative calculation by ^{1}H NMR determining sampled aliquots at different time intervals, presented by plots of numbers of monomer enchained, mass of CO_2 in polyols, and carbonate linkage, versus time. Reactions were carried out in the autoclave equipped with a sampling valve, with PO/[Al]/PPNCl=50000/1/1 &PO/SA=30 (molar ratio), 50 °C, 0.8/2.2 MPa CO_2 pressure, 25 mL PO in bulk. **c.** Plots of M_n versus time and GPC curves of sampled aliquots from 0.8 MPa reaction in **b**.

The double logarithmic plot of initial rates and PO concentration gave the reaction order in PO as the slope of the plot. As shown in Fig. 6b, a first-dependence for PO was clearly demonstrated in the concentration of 1.4-10.5 M in dichloromethane. This strongly suggests the ring-opening of PO attacked by the carbonate intermediate is the rate-determining step rather than CO_2 insertion into the alkoxide. Next, the plot of ln(k_{obs}) versus ln(cat) gave a slope of 0.9, indicating a first-order dependence in **CAT 1** within experimental error (Fig. 6c).[40] This stands in contrast to the order between 1 and 2 as observed in most mononuclear catalysts,[16] indicating the occurrence of intramolecular metal-metal cooperativity within one oligomeric catalyst chain as previously evidenced in the multinuclear Co(III) salen catalyzed hydrolytic kinetic resolution of epoxides[41,42] and a recent multimetallic CO_2/epoxide ROCOP catalysis[43]. To determine the activation energy (E_a), initial rates were measured in **CAT 1** involved controlled experiments at 50 °C, 60 °C, 70 °C, 80 °C, respectively. Fig. 6d depicted the Arrhenius plots for the formation of PPC while the absorption at *Ca.* 1800 cm^{-1} for cPC was not observable in such temperature range. The E_a for PPC was 34.2 kJ/mol in the presence of **CAT 1**, while **mono 1** showed significant higher E_a value of 44.7 kJ/mol for PPC (Fig. S51). The ΔE_a of 10.5 kJ/mol correlates well with the differentiated catalytic performance as observed before.

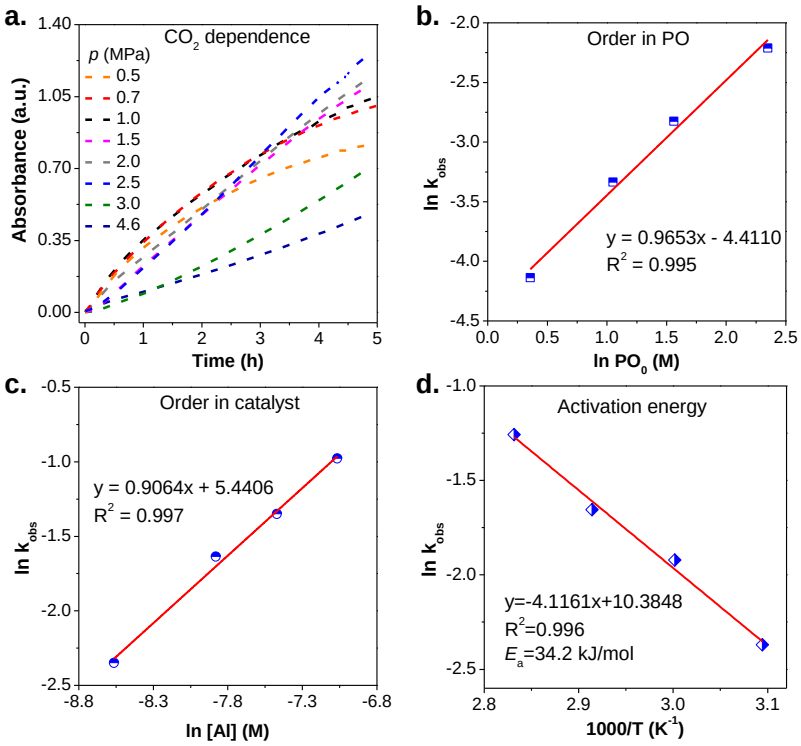

Figure 6. Kinetics studies of **CAT 1** for the formation of PPC determined by *in situ* IR. **a.** The dependence of initial rates on CO_2 pressure. **b.** Order in PO. **c.** Order in catalyst. **d.** Arrhenius plot.

In addition to Arrhenius method, the Eyring analysis was also involved to determine the activation parameters for further insight into the catalysis (Fig. S53).[44,45] With **CAT 1** (Fig. S49), the enthalpy of activation ($\Delta H^{\ddagger}$) values for PPC and PPO were determined to be 31.4, 42.0 kJ/mol and the entropy of activation ($\Delta S^{\ddagger}$) values for PPC and PPO were -167.9, -144.3 J/(mol*K), respectively. Overall, the transition state Gibbs free energy ($\Delta G^{\ddagger}$) values were 89.0 kJ/mol for PPC and 91.5 kJ/mol for PPO (at 70 °C). This similarity in $\Delta G^{\ddagger}$ values support the fact that **CAT 1** exhibits comparative rates of ROP and ROCOP from a thermodynamic perspective. Classic metal complexes like porphyrin and salen catalysts

normally produce polycarbonates with trivial ether linkage, while in striking difference, oligomeric **CAT 1** can produce ether-rich CO_2-polyols which extends the employment of metal-based CO_2 ROCOP catalysts previously only for biodegradable plastics to the manufacturing of polyurethanes. For comparison, the Eyring analysis was also applied for the case of **mono 1** in similar controlled temperature-dependent experiments achieving the following activation parameters for PPC: $\Delta H^{\ddagger}$ of 41.9 kJ/mol, $\Delta S^{\ddagger}$ of -158.4 J/(mol*K) and $\Delta G^{\ddagger}$ (at 70 °C) of 96.2 kJ/mol (Fig. S52). Since CO_2 is zero-order dependence in PPC formation, these activation parameters are supposed to be consistent with the transition state involving a carbonate end attacking the activated PO (Fig. S54). With **mono 1** the replacement of carbonate by PO in the coordinating site and the ring-opening of PO by carbonate proceed within one metal, while **CAT 1** allows that both anionic carbonate and PO are well stabilized in an intra- bimetallic manner and such Al-Al synergy is just a random permutation along the oligomeric chain. Such difference is substantiated by the $\Delta H^{\ddagger}$ value which is largely related to the stability of such transition state. The reduced enthalpy barrier with **CAT 1** accelerates the PO ring-opening step which leads to the high activity of the whole catalysis. On the other hand, the oligomer catalyst **CAT 1** accumulates monomers and propagating chains in a confined space, which decreases the degrees of freedom resulting in more entropic loss. Nevertheless, in the range of common operating temperature (25-100 °C), the use of **CAT 1** is always thermodynamically favored and $\Delta(\Delta G^{\ddagger})$ of **CAT 1** and **mono 1** is 6.9-7.6 kJ/mol due to the remarkable enthalpic benefit.

In general, quantitative CO_2 polymerization faces overlapped difficulties from low CO_2 pressure, the requirement of full conversion, and the use of protic compounds. The above discussion explains how **CAT 1** facilitates the transformation of quantitative CO_2 into polyols. Last but not least, another question is how to preserve such transformation afterwards, *i.e.*, why **CAT 1** realizes the switch catalysis from ROCOP to ROP while **mono 1** shifted to back-biting reaction under the same condition. To this end, the activation parameters with **mono 1** at the late stage were also studied. As shown in Fig. 7, when CO_2 is insufficient at the late stage, the catalytic resting state stalls at metal-alkoxide (*RS*), where three pathways may occur subsequently in the presence of excess PO as the monomer and solvent at the same time. In Path A, *RS* undergoes 1) the dissociation of polyol from the metal and 2) intramolecular "back-biting" between alkoxide end and adjacent carbonyl to give *TS A*. At last, cPC is afforded after releasing the remained chain which is likely to be coordinated back to the metal center or to diffuse into the bulk solution. With **mono 1**, the values of $\Delta H^{\ddagger}$ and $\Delta G^{\ddagger}$ (at 70 °C) were measured to be 40.5, 87.7 kJ/mol for such depolymerization. These activation parameters are significantly lower compared to those for initial cPC formation (the values of $\Delta H^{\ddagger}$ and $\Delta G^{\ddagger}$ at 70 °C were 57.9, 96.6 kJ/mol) under the same catalyst. The values are in line with the result where cPC is formed much faster by depolymerization from PPC at the late stage than coupling reaction in the beginning. In Path B, the alkoxide is first substituted by a new PO from the coordinating site and then directly attack it to realize enchainment. The activation parameters to reach *TS B* with **mono 1** were much higher: $\Delta H^{\ddagger}$ of 55.0 kJ/mol, $\Delta G^{\ddagger}$ (at 70 °C) of 100.7 kJ/mol. As evidenced in the kinetic studies with **mono 1**, the PO enchainment via Path B is dominated by the depolymerization via Path A. In sharp contrast, in Path C, **CAT 1** reached *TS C* with $\Delta H^{\ddagger}$ of 42.0 kJ/mol, $\Delta G^{\ddagger}$ (at 70 °C) of 91.5 kJ/mol as mentioned before, which was much lower than those of monometallic Path B. The reduced enthalpy is still the main contributor, since **CAT 1** with multiple Al centers assures the involvement of two metals (one for PO activation and another for the stabilization of the alkoxide end) in the attack of PO which effectively stabilizes the anionic transition state *TS C*. A previous literature even reported that the shorter distanced bimetallic pathway had more prominent promotion in PO ROP than PO/CO_2 ROCOP.[46] Therefore, **CAT 1** successfully shifts to ROP process from *RS* via Path C and thus sequesters the before-polymerized CO_2 once for all. Besides, from a macroscopic perspective, a feature of catalytic chain-transfer polymerization is that one metal serves as the active site for multiple propagation events,[47] which

greatly amplifies the diversity since free-base chains are more unstable and prone to depolymerize as previously illustrated by Darensbourg.[48] Hence, the isolated active sites also cause such uncontrolled catalysis in the presence of common mononuclear catalyst like **mono 1**. In terms of **CAT 1**, the loading is more extreme which results in one metal versus *Ca.* 1,000 polyols (Table 1). Nevertheless, the accumulation effect of **CAT 1** creates more possibilities for bimetallic interactions, and thus the swap between dormant chains and activated chains is tremendously accelerated which also stabilizes the dormant chains from "back-biting".

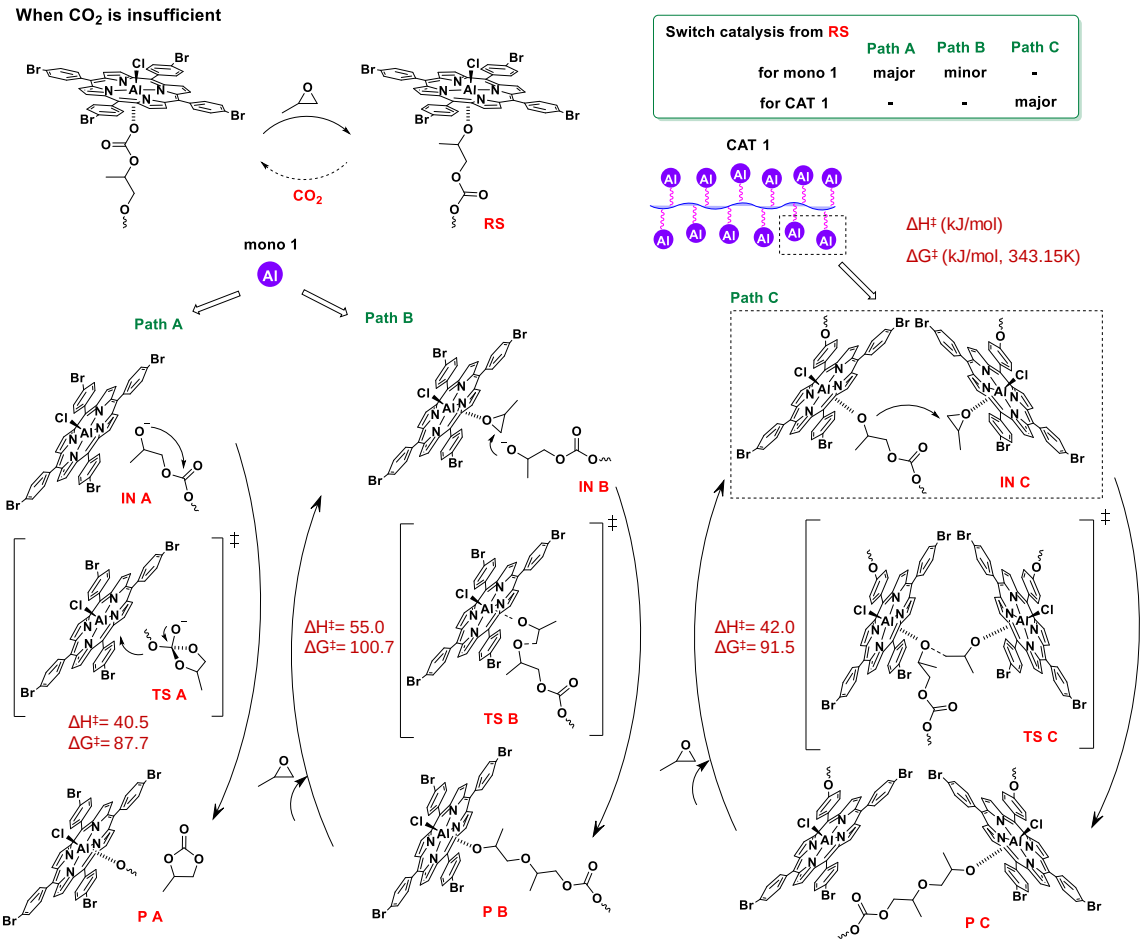

Figure 7. Proposed pathways from Al-alkoxide resting state at high CO_2 conversion.

Conclusion

Different from high pressure condition normally required in CO_2 transformation, and also different from the pursuit of absolute ambient pressure reaction, we establish an on-demand CO_2 fixation, which is the first time for quantitative CO_2 polymerization, tuning the composition of polyols by accurate CO_2 feed. Kinetic study reveals that under substoichiometric CO_2, **CAT 1** allows the *in situ* switch catalysis between CO_2-involved copolymerization and PO ROP when CO_2 was fully reacted, while common mononuclear catalysts shift the selectivity at high CO_2 conversion producing a mixture of polyol and cyclic carbonate. The success is attributed to the intra- multimetallic cooperativity of **CAT 1**, which increases the rate of monomer enchainment, stabilizes the key intermediates and blocks the "back-biting" pathway. The findings presented here provide mutual benefit for quantitative CO_2 transformation and precise polymer synthesis, which also elicits a question how precise catalysis can offer better opportunities for the development of green chemistry.

Data availability

Detailed experimental procedures, the characterization of all the synthesized compounds and polymers, other data mentioned in the manuscript are provided in the Supporting Information.

Author information

Corresponding Author

*E-mail: xhwang@ciac.ac.cn (X.W.).

ORCID identification number(s)

Xianhong Wang: 0000-0002-4228-705X

Conflict of interest

The authors declare no competing financial interest.

Acknowledgement

The authors greatly appreciated the financial support from Fundamental Science Center projector in National Natural Science Foundation of China (Grant No. 51988102) and Key Research Program of Frontier Sciences, CAS (Grant No .QYZDJ-SSW-JSC017).

References:

1 Hepburn, C. *et al.* The technological and economic prospects for CO_2 utilization and removal. *Nature* **575**, 87-97 (2019).

2 Artz, J. *et al.* Sustainable Conversion of Carbon Dioxide: An Integrated Review of Catalysis and Life Cycle Assessment. *Chem. Rev.* **118**, 434-504 (2018).

3 Mahoutian, M. & Shao, Y. Production of cement-free construction blocks from industry wastes. *J. Clean. Prod.* **137**, 1339-1346 (2016).

4 Song, Q. W., Zhou, Z. H., Yin, H. & He, L. N. Silver(I)-Catalyzed Synthesis of β-Oxopropylcarbamates from Propargylic Alcohols and CO_2 Surrogate: A Gas-Free Process. *ChemSusChem* **8**, 3967-3972 (2015).

5 De Luna, P. *et al.* Catalyst electro-redeposition controls morphology and oxidation state for selective carbon dioxide reduction. *Nat. Catal.* **1**, 103-110 (2018).

6 Zheng, X. *et al.* Theory-guided Sn/Cu alloying for efficient CO_2 electroreduction at low overpotentials. *Nat. Catal.* **2**, 55-61 (2019).

7 Klaus, S., Lehenmeier, M. W., Anderson, C. E. & Rieger, B. Recent advances in CO_2/epoxide copolymerization—New strategies and cooperative mechanisms. *Coord. Chem. Rev.* **255**, 1460-1479 (2011).

8 Nakano, R., Ito, S. & Nozaki, K. Copolymerization of carbon dioxide and butadiene via a lactone intermediate. *Nat. Chem.* **6**, 325-331 (2014).

9 Huang, R. *et al.* Deciphering key intermediates in the transformation of carbon dioxide into heterocyclic products. *Nat. Catal.* **2**, 62-70 (2019).

10 Qin, Y., Guo, H., Sheng, X., Wang, X. & Wang, F. An aluminum porphyrin complex with high activity and selectivity for cyclic carbonate synthesis. *Green Chem.* **17**, 2853-2858 (2015).

11 Sujith, S., Min, J. K., Seong, J. E., Na, S. J. & Lee, B. Y. A Highly Active and Recyclable Catalytic System for

CO_2/Propylene Oxide Copolymerization. *Angew. Chem. Int. Ed.* **47**, 7306-7309 (2008).

12 Anastas, P. & Eghbali, N. Green Chemistry: Principles and Practice. *Chem. Soc. Rev.* **39**, 301-312 (2010).

13 Burkart, M. D., Hazari, N., Tway, C. L. & Zeitler, E. L. Opportunities and Challenges for Catalysis in Carbon Dioxide Utilization. *ACS Catal.* **9**, 7937-7956 (2019).

14 Langanke, J. *et al.* Carbon dioxide (CO_2) as sustainable feedstock for polyurethane production. *Green Chem.* **16**, 1865-1870 (2014).

15 Deacy, A. C., Moreby, E., Phanopoulos, A. & Williams, C. K. Co(III)/Alkali-Metal(I) Heterodinuclear Catalysts for the Ring-Opening Copolymerization of CO_2 and Propylene Oxide. *J. Am. Chem. Soc.* **142**, 19150-19160 (2020).

16 Moore, D. R., Cheng, M., Lobkovsky, E. B. & Coates, G. W. Mechanism of the Alternating Copolymerization of Epoxides and CO_2 Using β-Diiminate Zinc Catalysts: Evidence for a Bimetallic Epoxide Enchainment. *J. Am. Chem. Soc.* **125**, 11911-11924 (2003).

17 Jutz, F., Buchard, A., Kember, M. R., Fredriksen, S. B. & Williams, C. K. Mechanistic Investigation and Reaction Kinetics of the Low-Pressure Copolymerization of Cyclohexene Oxide and Carbon Dioxide Catalyzed by a Dizinc Complex. *J. Am. Chem. Soc.* **133**, 17395-17405 (2011).

18 Yang, G.-W., Zhang, Y.-Y., Xie, R. & Wu, G. P. Scalable Bifunctional Organoboron Catalysts for Copolymerization of CO_2 and Epoxides with Unprecedented Efficiency. *J. Am. Chem. Soc.* **142**, 12245-12255 (2020).

19 Qin, Z. Q., Thomas, C. M., Lee, S. & Coates, G. W. Cobalt-based complexes for the copolymerization of propylene oxide and CO_2: Active and selective catalysts for polycarbonate synthesis. *Angew. Chem. Int. Ed.* **42**, 5484-5487 (2003).

20 Lu, X.-B. *et al.* Design of Highly Active Binary Catalyst Systems for CO_2/Epoxide Copolymerization: Polymer Selectivity, Enantioselectivity, and Stereochemistry Control. *J. Am. Chem. Soc.* **128**, 1664-1674 (2006).

21 Nakano, K., Kamada, T. & Nozaki, K. Selective Formation of Polycarbonate over Cyclic Carbonate: Copolymerization of Epoxides with Carbon Dioxide Catalyzed by a Cobalt(III) Complex with a Piperidinium End-Capping Arm. *Angew. Chem. Int. Ed.***45**, 7274-7277 (2006).

22 Robertson, N. J. *et al.* Two-dimensional double metal cyanide complexes: highly active catalysts for the homopolymerization of propylene oxide and copolymerization of propylene oxide and carbon dioxide. *Dalton Trans.* 5390-5395 (2006).

23 Liu, S. J., Qin, Y. S., Chen, X. S., Wang, X. H. & Wang, F. S. One-pot controllable synthesis of oligo(carbonate-ether) triol using a Zn-Co-DMC catalyst: the special role of trimesic acid as an initiation-transfer agent. *Polym. Chem.* **5**, 6171-6179 (2014).

24 Subhani, M. A., Kohler, B., Gurtler, C., Leitner, W. & Müller, T. E. Transparent Films from CO_2-Based Polyunsaturated Poly(ether carbonate)s: A Novel Synthesis Strategy and Fast Curing. *Angew. Chem. Int. Ed.* **55**, 5591-5596 (2016).

25 Deacy, A. C., Kilpatrick, A. F. R., Regoutz, A. & Williams, C. K. Understanding metal synergy in heterodinuclear catalysts for the copolymerization of CO_2 and epoxides. *Nat. Chem.* **12**, 372-380 (2020).

26 Nagae, H. *et al.* Lanthanide Complexes Supported by a Trizinc Crown Ether as Catalysts for Alternating Copolymerization of Epoxide and CO_2: Telomerization Controlled by Carboxylate Anions. *Angew. Chem. Int. Ed.* **57**, 2492-2496 (2018).

27 Cao, H., Qin, Y., Zhuo, C., Wang, X. & Wang, F. Homogeneous Metallic Oligomer Catalyst with Multisite Intramolecular Cooperativity for the Synthesis of CO_2-Based Polymers. *ACS Catal.* **9**, 8669-8676 (2019).

28 Sugimoto, H., Aida, T. & Inoue, S. Ring-opening polymerizations of lactone and epoxide initiated with aluminum complexes of substituted tetraphenylporphyrins. Molecular design of highly active initiators. *Macromolecules* **23**, 2869-2875 (1990).

29 Deng, J. *et al.* Aluminum porphyrins with quaternary ammonium halides as catalysts for copolymerization of cyclohexene oxide and CO_2: metal–ligand cooperative catalysis. *Chem. Sci.* **11**, 5669-5675 (2020).

30 Subhani, M. A., Gürtler, C., Leitner, W. & Müller, T. E. Nanoparticulate TiO_2-Supported Double Metal Cyanide Catalyst for the Copolymerization of CO_2 with Propylene Oxide. *Eur. J. Inorg. Chem.* **2016**, 1944-1949 (2016).

31 Gao, Y. G., Gu, L., Qin, Y. S., Wang, X. H. & Wang, F. S. Dicarboxylic acid promoted immortal copolymerization for controllable synthesis of low-molecular weight oligo(carbonate-ether) diols with tunable carbonate unit content. *J. Polym. Sci., Part A: Polym. Chem.* **50**, 5177-5184 (2012).

32 Meys, R., Katelhon, A. & Bardow, A. Towards sustainable elastomers from CO_2: life cycle assessment of carbon capture and utilization for rubbers. *Green Chem.* **21**, 3334-3342 (2019).

33 Pohl, M. *et al.* Dynamics of Polyether Polyols and Polyether Carbonate Polyols. *Macromolecules* **49**, 8995-9003 (2016).

34 Gong, R. *et al.* Terminal Hydrophilicity-Induced Dispersion of Cationic Waterborne Polyurethane from CO_2-Based Polyol. *Macromolecules* **53**, 6322-6330 (2020).

35 Schömer, M., Seiwert, J. & Frey, H. Hyperbranched Poly(propylene oxide): A Multifunctional Backbone-Thermoresponsive Polyether Polyol Copolymer. *ACS Macro Lett.* **1**, 888-891 (2012).

36 Na, S. J. *et al.* Elucidation of the Structure of a Highly Active Catalytic System for CO_2/Epoxide Copolymerization: A salen-Cobaltate Complex of an Unusual Binding Mode. *Inorg. Chem.* **48**, 10455-10465 (2009).

37 Asano, S., Aida, T. & Inoue, S. 'Immortal' polymerization. Polymerization of epoxide catalysed by an aluminium porphyrin–alcohol system. *J. Chem. Soc., Chem Commun*. 1148-1149 (1985).

38 Stößer, T., Sulley, G. S., Gregory, G. L. & Williams, C. K. Easy access to oxygenated block polymers via switchable catalysis. *Nat. Commun.* **10**, 2668 (2019).

39 Lehenmeier, M. W. *et al.* Flexibly tethered dinuclear zinc complexes: a solution to the entropy problem in CO_2/epoxide copolymerization catalysis? *Angew. Chem. Int. Ed.* **52**, 9821-9826 (2013).

40 Thevenon, A. *et al.* Indium Catalysts for Low-Pressure CO_2/Epoxide Ring-Opening Copolymerization: Evidence for a Mononuclear Mechanism? *J. Am. Chem. Soc.* **140**, 6893-6903 (2018).

41 Ready, J. M. & Jacobsen, E. N. Highly Active Oligomeric (salen)Co Catalysts for Asymmetric Epoxide Ring-Opening Reactions. *J. Am. Chem. Soc.* **123**, 2687-2688 (2001).

42 Zhu, X., Venkatasubbaiah, K., Weck, M. & Jones, C. W. Kinetic Evaluation of Cooperative [Co(salen)] Catalysts in the Hydrolytic Kinetic Resolution of rac-Epichlorohydrin. *ChemCatChem* **2**, 1252-1259 (2010).

43 Asaba, H. *et al.* Alternating Copolymerization of CO_2 and Cyclohexene Oxide Catalyzed by Cobalt–Lanthanide Mixed Multinuclear Complexes. *Inorg. Chem.* **59**, 7928-7933 (2020).

44 Switzer, J. M. *et al.* Quantitative Modeling of the Temperature Dependence of the Kinetic Parameters for Zirconium Amine Bis(Phenolate) Catalysts for 1-Hexene Polymerization. *ACS Catal.* **8**, 10407-10418 (2018).

45 Darensbourg, D. J., Moncada, A. I., Choi, W. & Reibenspies, J. H. Mechanistic Studies of the Copolymerization

Reaction of Oxetane and Carbon Dioxide to Provide Aliphatic Polycarbonates Catalyzed by (Salen)CrX Complexes. *J. Am. Chem. Soc.* **130**, 6523-6533 (2008).

46 Ohkawara, T., Suzuki, K., Nakano, K., Mori, S. & Nozaki, K. Facile estimation of catalytic activity and selectivities in copolymerization of propylene oxide with carbon dioxide mediated by metal complexes with planar tetradentate ligand. *J. Am. Chem. Soc.* **136**, 10728-10735 (2014).

47 Li, Y. *et al.* Carbon dioxide-based copolymers with various architectures. *Prog. Polym. Sci.* **82**, 120-157 (2018).

48 Darensbourg, D. J. Comments on the depolymerization of polycarbonates derived from epoxides and carbon dioxide: A mini review. *Polym. Degrad. Stab.* **149**, 45-51 (2018).

Table of Contents